



**HAL**  
open science

# Influence of the Oxygen Partial Pressure on the High Temperature Corrosion of A 38Ni-34Fe-25Cr Steel in Presence of NaCl Salt

L. Couture, Francois Ropital, François Grosjean, J. Kittel, V. Parry, Y. Wouters

► **To cite this version:**

L. Couture, Francois Ropital, François Grosjean, J. Kittel, V. Parry, et al.. Influence of the Oxygen Partial Pressure on the High Temperature Corrosion of A 38Ni-34Fe-25Cr Steel in Presence of NaCl Salt. International Conference on high temperature corrosion and protection of metals (HTCPM), May 2012, Les Embiez, France. hal-02474924

**HAL Id: hal-02474924**

**<https://ifp.hal.science/hal-02474924>**

Submitted on 11 Feb 2020

**HAL** is a multi-disciplinary open access archive for the deposit and dissemination of scientific research documents, whether they are published or not. The documents may come from teaching and research institutions in France or abroad, or from public or private research centers.

L'archive ouverte pluridisciplinaire **HAL**, est destinée au dépôt et à la diffusion de documents scientifiques de niveau recherche, publiés ou non, émanant des établissements d'enseignement et de recherche français ou étrangers, des laboratoires publics ou privés.

# Influence Of The Oxygen Partial Pressure On The High Temperature Corrosion Of A 38Ni-34Fe-25Cr Steel In Presence Of NaCl Salt

L. Couture<sup>a,b</sup>, F. Ropital<sup>b</sup>, F. Grosjean<sup>b</sup>, J. Kittel<sup>b</sup>, V. Parry<sup>a</sup>, Y. Wouters<sup>a</sup>

<sup>a</sup>*SIMaP, Grenoble-INP / UJF / CNRS, BP 75, 38402 Saint Martin d'Hères cedex, France*

<sup>b</sup>*IFP Énergies nouvelles, Rond Point de l'échangeur de Solaize BP3, 69360 Solaize, France*

[ludovic.couture@yahoo.fr](mailto:ludovic.couture@yahoo.fr), [francois.ropital@ifpen.fr](mailto:francois.ropital@ifpen.fr), [francois.grosjean@ifpen.fr](mailto:francois.grosjean@ifpen.fr), [jean.kittel@ifpen.fr](mailto:jean.kittel@ifpen.fr),  
[yves.wouters@simap.grenoble-inp.fr](mailto:yves.wouters@simap.grenoble-inp.fr), [Valerie.Parry@simap.grenoble-inp.fr](mailto:Valerie.Parry@simap.grenoble-inp.fr)

**Abstract.** In biomass gasification process, some molten salts of the feed can generate high temperature corrosions. In this study the chromia-forming austenitic alloy Haynes<sup>®</sup> HR-120 was oxidized with a deposit of sodium chloride during 96 hours at 825°C and 900°C. Two different atmospheres were selected; one with a high oxygen partial pressure (Ar/O<sub>2</sub> 90/10 %vol.) and one, named syngas, with a low oxygen partial pressure (CO/H<sub>2</sub>/CO<sub>2</sub> 45/45/10 %vol.). While at 900°C the behaviour of the alloy in presence of sodium chloride was catastrophic in high oxidizing conditions, the impact of sodium chloride was insignificant in the other atmosphere. Under Ar/O<sub>2</sub> mixture, the catastrophic oxidation was attributed to the setting up of an active oxidation. At 900°C under syngas atmosphere, the protective behaviour of the alloy seems linked to the association of a faster evaporation of the salt and a very low oxygen partial pressure. At 825°C a catastrophic behaviour is observed under syngas atmosphere as the NaCl evaporation rate is much slower.

**Keywords:** Catastrophic oxidation, active oxidation, NaCl, low oxygen partial pressure

## 1 INTRODUCTION

In modern power plants, the partial pressure of oxygen in combustion atmosphere may be extremely low. Combustion under reducing atmospheres can occur in gasification plants [1], in low-NO<sub>x</sub> plants [2], in recovery boilers [3, 4], and also locally in other boilers due to incompletely oxidized flue gases [5].

This study focuses on material issues in high temperature technologies where low oxygen levels occur. Processes of interest include gasification of waste, black liquor and biomass, which may be used in conjunction with gas turbines for power production, or as a synthetic gas (syngas) feed to GTL (gas-to-liquid) processes to produce liquid fuels. Syngas produced by gasification process of biomass fuels is an environmental friendly alternative to conventional petrochemical fuels for the production of electricity, hydrogen and other chemicals, or for the partial replacement of gasoline for car engines.

However, using biomass for syngas production is not straightforward. One of the major issue lies on the high concentration of salts in vegetal residues. In the convective pass of a boiler, the flue gas is cooled down and some of the alkali metals and salts may condense on the heat exchanger tubes, resulting in severe risks of corrosion [6, 7][6, 7]. In addition, contaminants can also deactivate the catalysts used for downstream reaction such as steam reforming methane or Fischer–Tropsch synthesis [8].

The impact of chlorine on corrosion of refractory alloys has already been studied by several authors [1, 7, 9, 10]. A common hypothesis regarding chlorine-induced high temperature corrosion is that chlorine may cause a direct corrosion by accelerating the oxidation of metals and alloys. This phenomenon is often referred as “active oxidation” [7, 10]. High chromium alloys are considered to form a protective oxide scale even in low-partial

pressure of oxygen. In the presence of chlorine, these alloys suffer strong corrosion [11]. Nickel based alloys usually present better resistance against chloridation. This behaviour is explained by the partial pressure of nickel chloride being significantly lower than partial pressure of iron chlorides and the Gibbs free energy change of NiCl<sub>2</sub> formation is less negative than that of FeCl<sub>2</sub> formation. Indeed, vapour transport of metal chlorides often plays a critical role in chloride-induced corrosion mechanisms [9, 10]

In the present work, the effect of sodium chloride on the chromia-forming HR-120 alloy (38Ni-34Fe-25Cr) is evaluated in a simulated process atmosphere CO/H<sub>2</sub>/CO<sub>2</sub> (45/45/10 %vol.) at 825 and 900°C during 96 hours. As a limited number of information are available from the literature under low oxygen partial pressure conditions, a high oxidizing atmosphere: Ar/O<sub>2</sub> (90/10 %vol.) was also selected as a reference.

## 2 EXPERIMENTAL

### 2.1 Samples and spray procedure

The material used in this study is the austenitic alloy Haynes<sup>®</sup> HR-120. Its chemical composition is shown in TABLE 1. Specimens of 20 × 10 mm<sup>2</sup> were cut from a 1 mm thick sheet. Specimens were ground from 320 SiC grit to a 1200 SiC grit finish and finally rinsed with distilled water.

TABLE 1 Chemical composition of HR-120 (wt%)

Fe	Ni	Cr	Co	Mo	W	Nb	Mn	Si	Al	C	B
34.34	37.97	25.17	0.11	0.34	0.08	0.61	0.77	0.41	0.06	0.05	0.002

Prior to carrying out oxidation runs, the samples were sprayed on all sides with an aqueous saturated solution of NaCl, leading to the formation of a network of salted drops. After a heating step in a furnace at 150°C during 15 minutes and cooling to room temperature, NaCl crystallites appeared on the surface, forming a network of square crystals (FIGURE 1). The average diameter of the crystals is in the range 20-100 μm and the mass of deposit is approximately 0.75 mg cm<sup>-2</sup>.

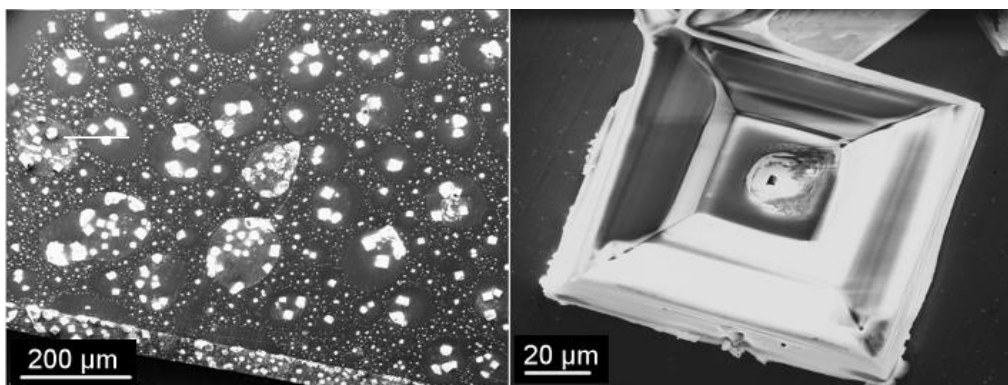


FIGURE 1 SEM surface view of NaCl salt particles after a heating step at 150°C

### 2.2 Experiments

Thermogravimetric analysis (TGA) tests were carried out on a Setaram TAG B24 apparatus in two different atmospheres: a flowing mixture of CO, H<sub>2</sub> and CO<sub>2</sub> respectively 45/45/10 %vol., representing the syngas environment with a low oxygen partial pressure; a flowing mixture of Ar and O<sub>2</sub> respectively 90/10 %vol., representing a highly oxidising reference media.

Prior to introducing the test gas mixture in the reactor, the samples were heated from room temperature up to 825 or 900°C at rate of 20°C min<sup>-1</sup> under argon in order to avoid any oxidation. When the target temperature was reached, the atmosphere was introduced into the reactor with a flow rate of 100 mL min<sup>-1</sup>. This regime was

maintained during 96 h. Then, the reactor was flushed with argon and the samples were cooled down to room temperature under this atmosphere to avoid any further reaction [11, 13].

## 2.3 Analysis

After oxidation, the samples were analyzed by X-Ray diffraction (XRD) and scanning electron microscope – energy dispersive spectroscopy (SEM-EDS) techniques. The X-ray diffractograms were obtained using Cu  $K_{\alpha}$  radiation of a Rigaku Miniflex II. Surface and transverse SEM views of the samples and EDS analysis were obtained with a LEO S440 Stereoscan instrument equipped with the EDAX Genesis software.

## 3 RESULTS

In order to precisely evaluate the composition of the high temperature environment, thermodynamic calculations were made using [FactSage 6.2, SGTE 2009] software.

When heated at 900°C, the syngas composed of 45% CO, 45% H<sub>2</sub>, 10% CO<sub>2</sub> at ambient temperature transforms into 50% CO, 40% H<sub>2</sub>, 5% CO<sub>2</sub>, 5% H<sub>2</sub>O with minor CH<sub>4</sub>.

In presence of salt at 900°C (molar composition ratio of 10<sup>5</sup> CO-H<sub>2</sub>-CO<sub>2</sub> / 1 NaCl), thermodynamic calculation gives the following partial pressures  $p(\text{NaCl}) = 2.1 \cdot 10^{-3}$  atm;  $p(\text{O}_2) = 8.1 \cdot 10^{-19}$  atm;  $p(\text{Cl}) = 4.2 \cdot 10^{-12}$  atm;  $p(\text{Cl}_2) = 1.4 \cdot 10^{-18}$  atm. The evaporation of sodium chloride will be very fast at 900°C.

For the oxidizing environment, (molar composition ratio 10<sup>5</sup> Ar-O<sub>2</sub> / 1 NaCl at ambient temperature) . . , the obtained partial pressure are:  $p(\text{NaCl}) = 2.1 \cdot 10^{-3}$  atm;  $p(\text{O}_2) = 0.10$  atm;  $p(\text{Cl}) = 1.8 \cdot 10^{-9}$  atm;  $p(\text{Cl}_2) = 2.4 \cdot 10^{-13}$  atm. The evaporation of sodium chloride will be also very fast at 900°C.

These phenomena are confirmed by the kinetic curve of NaCl evaporation at 900°C (FIGURE 2).

Thermodynamic evaluation was then extended to take into account the presence of metals. The thermodynamic stability of metal chlorides and oxides at a given temperature depends on the partial pressures of oxygen and chlorine. Thermodynamic phase stability diagrams were established at 900°C for the systems M-O-Cl with M = Cr, Fe, Ni (FIGURE 3). For both the low (syngas) and high oxidising atmospheres of our study, it can be seen that metal chlorides cannot be formed on the surface of the alloy. We can also determine that chromium oxide might form under both low and high oxygen partial pressure, while iron and nickel oxides are stable only in the high O<sub>2</sub> pressure situation.

However, chlorine can diffuse through the oxide layer, although the mode of transport of chlorine has not been clearly established [11]. Linked to the very low oxygen partial pressure prevailing in the vicinity of the substrate, the formation of metal chlorides is then possible. Metal chlorides have a high vapor pressures even at low temperatures, which can lead to vaporization and rapid loss of metal from the surface [7]. Several authors agree that volatilization becomes the corrosion dominant mechanism if the vapor pressure of a metal chloride exceeds 10<sup>-4</sup> atm [14, 15].

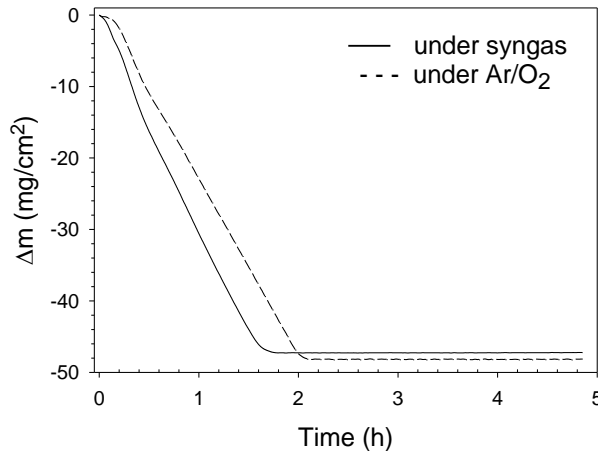


**FIGURE 2** TGA curve of a crucible with 50 mg of NaCl under Ar/O<sub>2</sub> and syngas atmosphere at 900°C

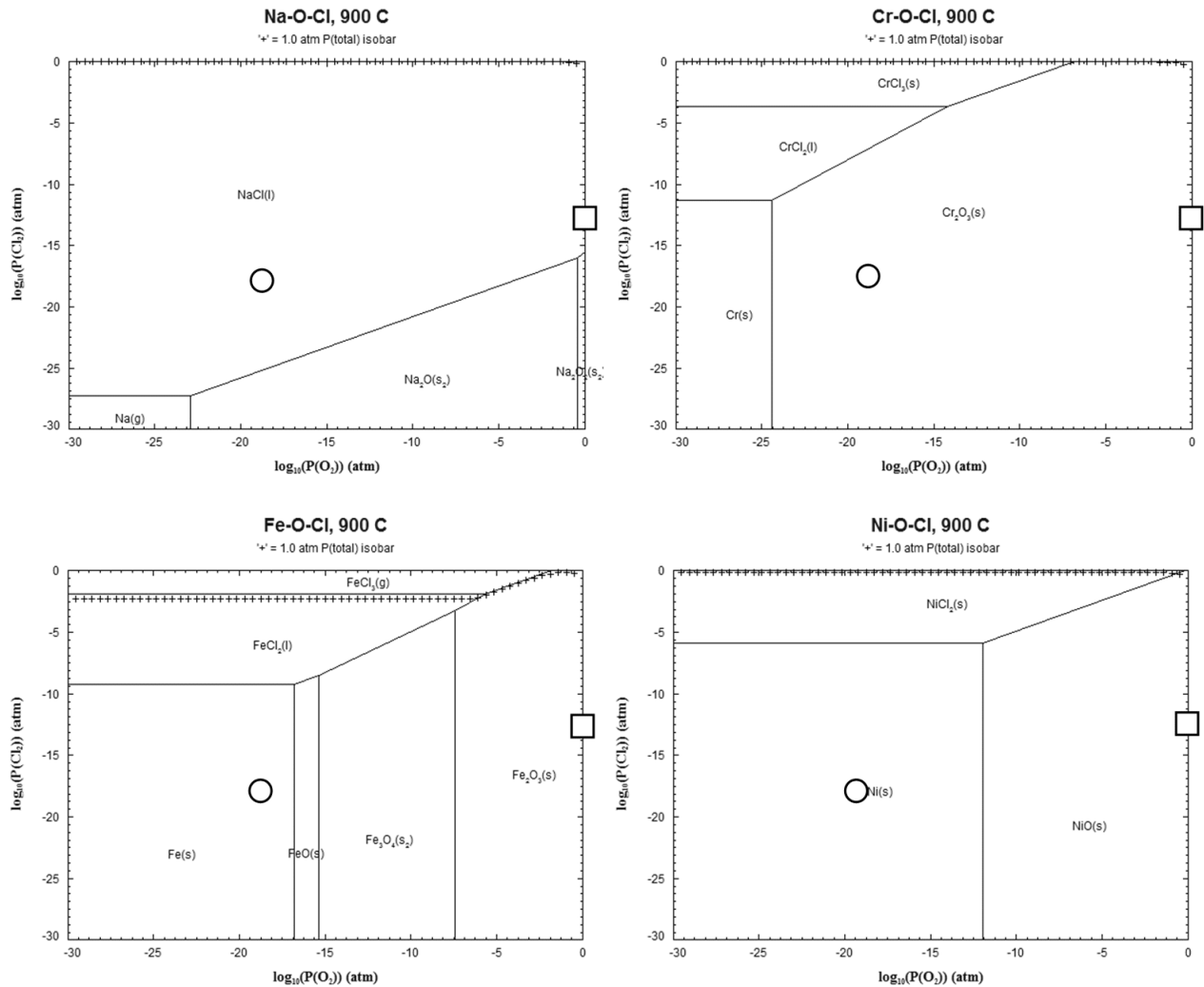


**FIGURE 3** Stability diagrams of Na-O-Cl (a), Cr-O-Cl (b), Fe-O-Cl (c) and Ni-O-Cl (d) at 900°C and  $P = P_{atm}$   
 Circle: Low oxidising atmosphere; Square: High oxidising atmosphere

The influence of NaCl on alloy HR-120 mass gain is illustrated in FIGURE 4a under the mixture Ar/O<sub>2</sub> and in FIGURE 4b under syngas atmosphere. Initially, a mass loss is observed during the five first minutes, linked to the evaporation of sodium chloride.

With high  $p(O_2)$ , we observe a strong rate of oxidation characterized by a significant increase of the mass gain (+ 13.6 mg.cm<sup>-2</sup> after 96 hours). The presence of sodium chloride induces a three-stage corrosion kinetic. During the 12 first hours, the mass gain follows a parabolic rate law, then moves on to a linear rate law with an oxidation rate of 0.12 mg.cm<sup>-2</sup>.h<sup>-1</sup> until 40 hours. After, there is a slight slowing down of the kinetic.

Kinetic oxidation of the alloy in presence of sodium chloride under very low oxygen partial pressure presents a very slight mass gain with a parabolic rate law. The value of the parabolic constant is  $k_p = 5.5 \cdot 10^{-4} \text{ mg}^2 \text{ cm}^{-4} \text{ h}^{-1}$ . After 96 hours, the mass gain is less than 0.20 mg.cm<sup>-2</sup>.

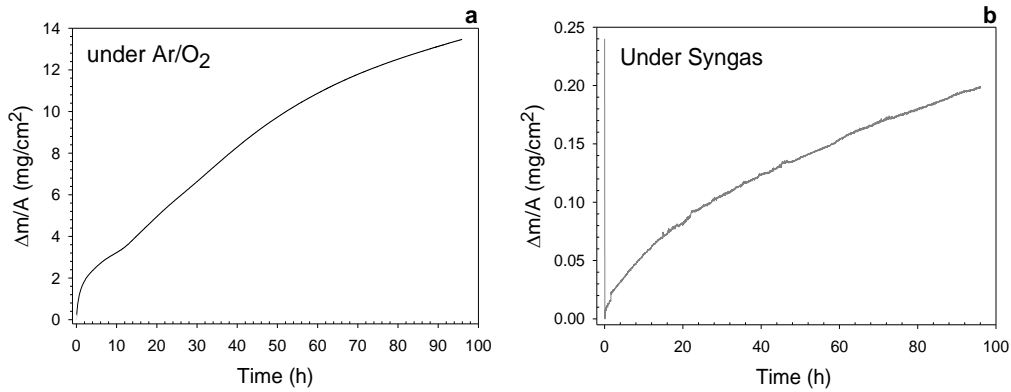


**FIGURE 4** TGA of HR-120 with sodium chloride at 900°C under high oxygen partial pressure (a), and under low oxygen partial pressure (b)

FIGURE 5 presents the X-ray diffraction analysis results of the corrosion products obtained after the exposition of HR-120 samples to both atmospheres in presence of salt deposit at 900°C during 96 hours. Diffraction peaks arising from the substrate ( $\gamma$  phase) are observed in both conditions. Taking into account the X-ray penetration, the intensity of the  $\gamma$  phase is higher under syngas atmosphere, that means a lower thickness of the corrosion layer, which is in good agreement with TGA results and SEM analysis presented below.

Under oxidizing atmosphere, the rhombohedral oxide solid solution ( $\text{Fe}_x\text{Cr}_{1-x}\text{O}_3$  (R phase) and the spinel-type oxide ( $\text{M}_{1-x}\text{Cr}_x\text{O}_4$  (with  $\text{M} = \text{Fe}$  or  $\text{Mn}$ ) (S phase) are identified. In addition, we note the formation of iron oxides as hematite (H phase) and magnetite (M phase). All these oxides are characteristic of the catastrophic oxidation of chromia forming alloys.

Under syngas atmosphere the X-ray diffraction analysis has identified only the presence of the rhombohedral oxide solid solution (R phase) and chromium-manganese or chromium iron spinel (S phase).

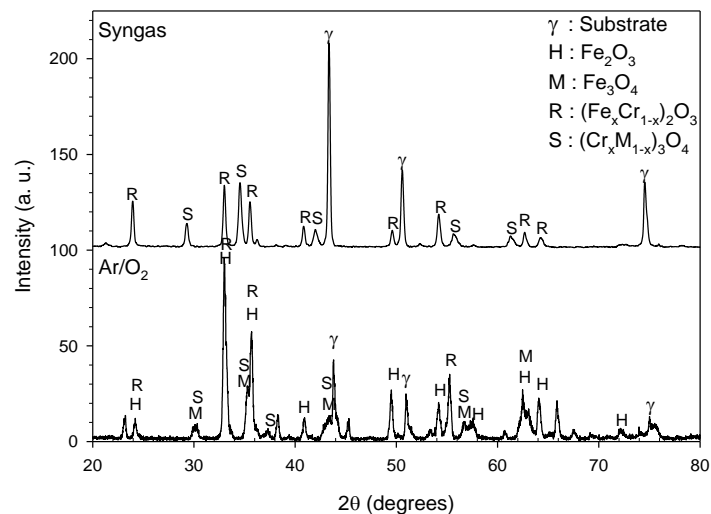


**FIGURE 5** XRD of HR-120 after 96 h at 900°C with sodium chloride under high and low oxygen partial pressure

The surface and cross-section morphologies of the oxide layer exhibited strong differences under the two conditions (high and low  $p(\text{O}_2)$ ). FIGURE 6a and b show the SEM surface view of HR-120 after a 96 h exposure at 900°C under the Ar/ $\text{O}_2$  atmosphere. We can observe different morphologies of crystals: cauliflower-shaped oxide, with diameter ranging from 5 to 25  $\mu\text{m}$ ; faceted oxides with triangular shape ranging in size from 1 to 2 microns; crystals with lower dimension, with no particular orientation or geometry. Lower magnification observations also indicate that the corrosion product suffered intensive spalling, reaching approximately 50 % of the area of the specimen. It has been noticed that during thermogravimetric result, spallation occurred mainly during cooling. Tilted views of the spalled scale (FIGURE 6c and d) show that the thickness is approximately 60  $\mu\text{m}$ . It also seems that the adherence is rather poor. Observations at higher magnification (FIGURE 6d) underline heterogeneities between internal and external parts of the oxide. At the interface with the substrate, the oxide is composed of small grains with a columnar morphology. Larger grains without preferential orientation are found at the outer part of the scale.

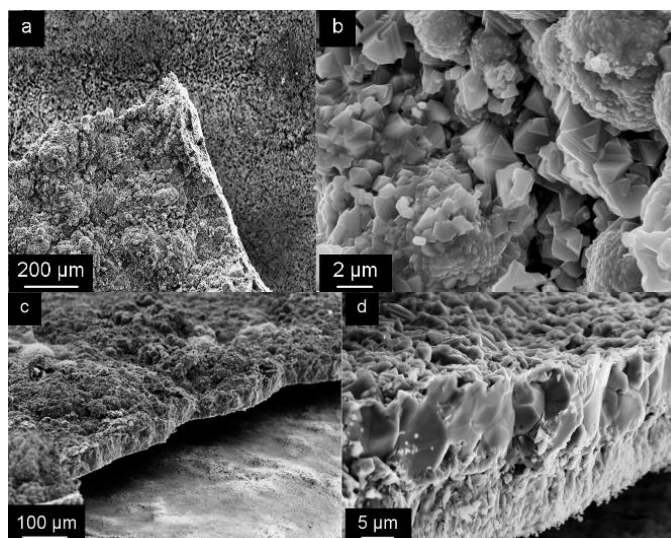


**FIGURE 6** SEM micrographies of HR-120 under high oxygen partial pressure at 900°C

FIGURE 7a and b show the SEM surface views of HR-120 after 96 h exposure at 900°C under syngas atmosphere. The surface is homogeneously composed of small crystallites and lamellas appearing along the grain boundaries of metal. Additionally, larger crystals are observed, with dimension and shape similar to sodium chloride crystals that were deposited on the surface before the experiments (FIGURE 1). However, EDX analyses of these crystals indicate that they are composed only of oxygen and chromium. The cross section of the specimen exposed under syngas atmosphere (FIGURE 7c), shows that the thickness of the oxide scale is in the range of 1 μm, in accordance with thermogravimetric measurements. Oxide scale seems to be dense, compact and adherent. Nevertheless, several occurrences of localized internal attack were also observed below the oxide scale.

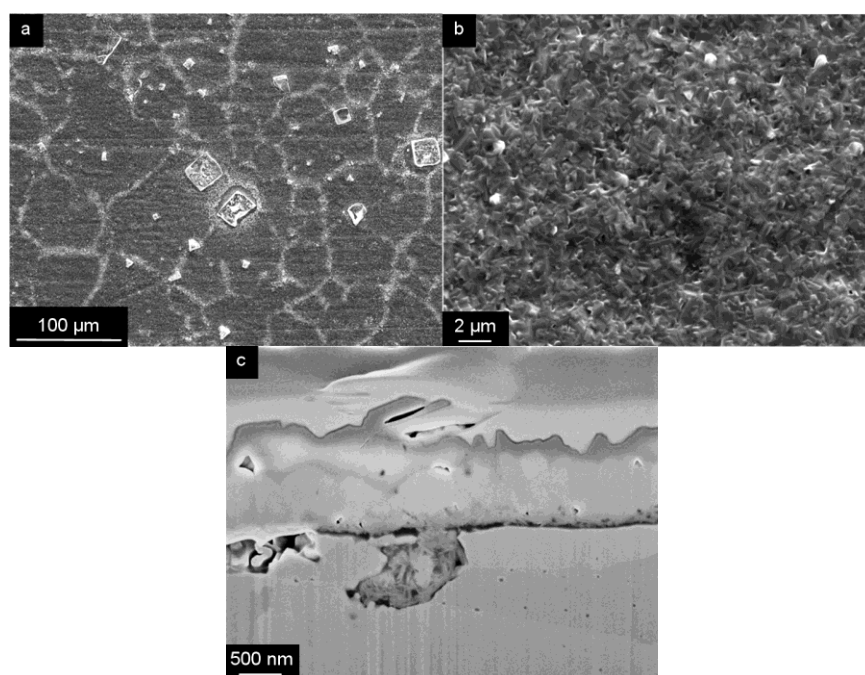


**FIGURE 7** SEM micrographies of HR-120 under low oxygen partial pressure at 900°C

In biomass gasification process, during the cooling of the flue gas, alkali salts may condense on the surfaces of heat exchanger tubes in a wide range of temperatures. A previous work was done on the effect of  $\text{Na}_2\text{SO}_4$  and was conducted at 900°C [16]. For this reason, the first part of this article concerns experiments performed at the same temperature. But, as 900°C is just above the melting temperature of the sulfate of sodium, it seemed interesting to carry out other tests at 825°C, a temperature which is just above the melting temperature of  $\text{NaCl}$  ( $T_{\text{melting}} = 801^\circ\text{C}$ ).

The impact of sodium chloride deposits towards alloy Haynes HR-120 under the syngas atmosphere at 825°C and 900°C is illustrated in FIGURE 8. The temperature has a strong influence on the mass gain which is seven times greater at 825°C than at 900°C. .

FIGURE 9 displays that the evaporation rate of sodium chloride is lower at 825°C than 900°C (32.8 mg.h<sup>-1</sup>.cm<sup>-2</sup> at 900°C and 3.1 mg.h<sup>-1</sup>.cm<sup>-2</sup> at 825°C). Thus, the contact time between the molten salt and the alloy at the beginning of the experiment will be greater at 825°C than 900°C, which may explain the TGA results.

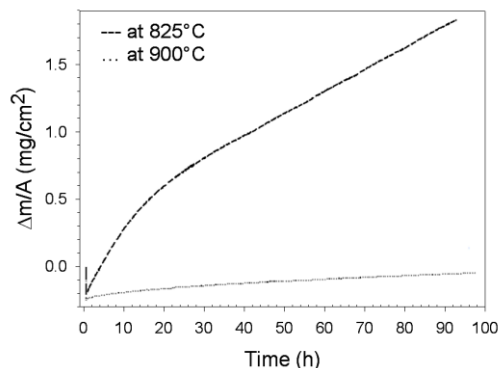


**FIGURE 8** Kinetic oxidation of HR-120 under syngas atmosphere in presence of sodium chloride

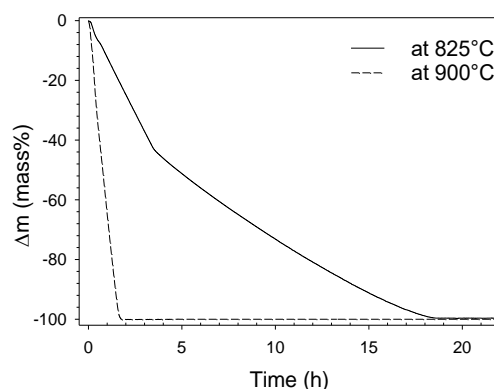


**FIGURE 9** Kinetic evaporation of sodium chloride under syngas atmosphere

## 4 DISCUSSION

From a kinetic, morphological and structural point of view, the impact of sodium chloride on the corrosion behaviour of alloy HR120 differs according to the selected atmospheres and temperatures.

At 900°C in presence of NaCl, thermogravimetric measurements under oxidizing atmosphere present a very strong mass gain whereas the mass gain is very slight under low oxidizing environment (syngas). Consequently, quick evaporation of sodium chloride which inevitably occurs within our test protocol is not the only argument to explain the protective behaviour of the alloy under syngas. In fact, at 900°C, the kinetic evaporation rate of sodium chloride is in the same range of magnitude under Ar/O<sub>2</sub> mixture or syngas atmosphere.

After corrosion tests with NaCl under the oxidizing atmosphere, the oxide scale is porous, non-adherent, non-continuous and non-protective. The oxide layer is mainly composed of magnetite and hematite which is typical to the catastrophic oxidation of austenitic alloys with high chromium and iron content [17]. Spallation of the oxide scale occurs during cooling and more than 50 % of the area of the specimen is thus spalled. This catastrophic behaviour of the alloy can be attributed to the presence of chlorine according to the well known « active oxidation » mechanism [18]. Haanappel *et al.* [19] indicate that both chlorine and water vapor are known to accelerate corrosion significantly by decreasing the density and integrity of the corrosion scales: chlorine prevents the formation of a protective oxide layers and accelerates the corrosion by an "active oxidation" mechanism. In this mechanism, molecular chlorine is supposed to generate volatile transition-metal chlorides at the scale/metal interface. The chlorides evaporate and diffuse towards the gas/scale interface. Within the scale, the oxygen partial pressure

increases and in the external parts of the scale, the oxygen partial pressure is high enough to transform the gaseous chlorides into solid oxides releasing gaseous chlorine and forming a non-protective scale. The chlorine returns partially to the scale/metal interface and a reaction circuit occurs in which chlorine acts as a catalyst, accelerating the oxidation [11].

One of the key steps is the transformation of metal chloride to metal oxide. Under very low oxygen partial pressure prevailing in the syngas atmosphere, iron and nickel oxides are thermodynamically unstable and the metal chlorides potentially formed cannot be oxidized, and, due to their high volatility they can be transported outside the oxide scale. Metal chlorides evaporated into the atmosphere. As within our experimental conditions the salt layer becomes depleted in chlorine and the oxide scale can recover a protective behaviour toward the syngas atmosphere.

However, the low oxygen partial pressure is not sufficient to obtain a protective behaviour of the alloy as observed with our test protocol (batch deposit of NaCl). Indeed, under syngas, the corrosion rate is greater at 825°C than at 900°C. As illustrated by the kinetic evaporation of NaCl, the duration of the contact between the alloy and the salt is probably lower at 900°C than at 825°C. At this latter temperature, the contact time is increased, resulting in a higher reactivity of the alloy with the atmosphere and a greater mass gain. Even a brief contact of few minutes between the salt and the alloy is enough to cause an irreversible catastrophic oxidation.

At 900°C, the protective behaviour of HR-120 alloy in presence of sodium chloride under syngas atmosphere can then be attributed to the association of two factors: fast evaporation of salt and a very low oxygen partial pressure. At 825°C, the slowest evaporation rate of the salt seems to an important parameter that leads to a much more higher corrosion rates than at 900°C.

## CONCLUSION

At 900°C the influence of sodium chloride on the corrosion behaviour of HR-120 alloy depends strongly on the atmosphere selected. While the corrosion of the alloy in presence of chlorine is catastrophic under oxidizing environment, the impact of sodium chloride seems to be insignificant under syngas atmosphere. Under Ar/O<sub>2</sub> mixture, our observations are in accordance with most of results published in the literature: the catastrophic oxidation seems to be governed by an active oxidation type mechanism. At 900°C under syngas atmosphere, protective behaviour of the alloy is associated to the combination of faster evaporation of salt and very low oxygen partial pressure. At 825°C a catastrophic behaviour is observed under syngas atmosphere as the NaCl evaporation rate is much slower.

## REFERENCES

1. V. Guttman, K. Stein, W.T. Bakker, *Mater. High Temp.*, **14**, 127(1997).
2. R.M. Deacon, J.N. DuPont, A.R. Marder, *Mater. Sci. Eng. A*, **460**, 392 (2007).
3. M.A. Uusitalo, P.M.J Vuoristo, T.A Mantyla, *Corros. Sci.*, **46**, 1311 (2004).
4. A. Klarin, *Tappi Journal* **76**, 183 (1993).
5. H. Kassman, M. Broström, M. Berg, L.E. Åmand, *Fuel* **90**, 1325 (2011).
6. D.J. Gooch, *Int. Mater. Rev.*, **45**, 1 (2000).
7. H.P. Nielsen, F.J. Frandsen, K. Dam-Johansen, L.L. Baxter, *Prog. Ener. Comb. Sci.*, **26**, 283 (2000)
8. X. Meng, W. de Jong, R. Pal, A.H.M. Verkooijen, *Fuel Process. Technol.*, **91**, 964 (2010)
9. S. Chevalier, S. Ched'Homme, A. Bekaddour, K. Amilain-Basset, L. Buisson, *Mater. Corros.*, **58**, 254 (2007).
10. A. Zahs, M. Spiegel, H.J. Grabke, *Corros. Sci.*, **42** 1093 (2000).
11. H.J. Grabke, E. Reese, M. Spiegel, *Corros. Sci.*, **37**, 1023 (1995).
12. F. Ropital, F. Bonnet, *Mater. Sci. Forum* **595**, 681 (2008).
13. F. Bonnet, F. Ropital, Y. Berthier and P. Marcus, *Mater. Corros.*, **54**, 870 (2003).
14. H.J. Grabke, Incinerating municipal and industrial waste, New York: Hemisphere (1989) p.161
15. E. Reese, H.J. Grabke, *Mater. Corros.*, **43**, 547 (1992).
16. L. Couture, F. Ropital, F. Grosjean, J. Kittel, V. Parry, Y. Wouters, *Corrosion Science* **55**, 133-139 (2012).
17. A. Galerie, S. Henry, Y. Wouters, M. Mermoux, J.P. Petit, L. Antoni, *Mater. High Temp.*, **22** 105 (2005).
18. Y. Shinata, F. Takahashi, K. Hashiura, *Mater. Sci. Eng. A*, **87**, 399 (1987).
19. V.A.C. Haanappel, T. Fransen, P.J. Gellings, *Corros. Sci.*, **48**, 812 (1992).